

# Calorimetric and Spectroscopic Investigation of the Acidity of HZSM-5

Russell S. Drago,\* Sílvia C. Dias,† Mariana Torrealba,‡ and Lola de Lima‡

Contribution from the Department of Chemistry, University of Florida,  
Gainesville, Florida 32611-7200

Received September 25, 1996<sup>⊗</sup>

**Abstract:** The cal-ad analysis of HZSM-5 provides a novel characterization of the donor-acceptor properties of this solid acid showing 0.0415 mmol per g of a strong Brønsted site and 0.53 mmol per g of a weaker site. Of all studies to date, only cal-ad provides a measure of the extent,  $K_i$ ; strength,  $-\Delta H_i$ ; and quantity of sites. The relative  $K$  values show why gas phase calorimetry, TPD, TGA, DSC, and isopropylamine decomposition do not resolve the two sites found by cal-ad and incorrectly suggest 0.6 mmol g<sup>-1</sup> of strong acid sites. Reaction with pyridine gives an enthalpy of 42.1 and 8.6 kcal mol<sup>-1</sup>, respectively, for the two sites suggesting the latter is a hydrogen bonding site. Other acidity measures average these sites, and their enthalpies contain dispersion as well as donor-acceptor components. Comparison of these results with other cal-ad results suggests HZSM-5 is a strong solid acid but not a super acid. Titrations with 2,6-lutidine and 2,6-di-*tert*-butylpyridine indicate that the strong Brønsted sites are located in the 5.5 Å channels with no detectable amounts on the exterior surface.

## Introduction

Solid acid catalysts are the most commonly used catalytic materials in the chemical industry.<sup>1</sup> Amongst solid acids, zeolites are most important in commercial processes finding applications not only in acid catalysis<sup>2</sup> but also in separation applications.<sup>3</sup> In spite of considerable effort, the measurement of acidity and the role that acidity plays in the catalyzed chemical conversions remain key problems in the solid acid area.<sup>4</sup> Reviews and other reports have discussed the inadequacies of Hammett indicators,<sup>5</sup> temperature programmed desorption (TPD), thermogravimetric analysis (TGA), and differential scanning calorimetry<sup>6</sup> as measures of acidity. Some of the more recent articles<sup>7,8</sup> in this area have employed solid-gas calorimetric measurements to measure acidity, and there are limited studies reporting calorimetric measurement of bases reacting with solid acids slurried in nonbasic solvents.<sup>9</sup> These calorimetric studies report enthalpies obtained by dividing the heat

evolved by the moles of limiting reagent. It is assumed that only the strongest sites react at low base concentration, but the enthalpies really are average enthalpies of all the sites to which the base coordinates. This average enthalpy is a measure of the acid strength of the strongest site only if just the strongest site reacts.

Recent reports from this laboratory<sup>10</sup> have described a cal-ad procedure for evaluating the acidity of solids which employs the combined measurements from adsorption studies and calorimetry to better define the solid-base (or acid) equilibria than is possible with the separate measurements. This procedure provides the equilibrium constant ( $K_{ad,i}$ ), the enthalpy ( $\Delta H_i$ ), and the number of acid sites ( $n_i$ ) for each of the  $i$ -different types of sites in the solid. The individual site contributions to the total heat are determined with the  $K$  values, so the assumption that only the strongest site is coordinated is not made. The resulting donor-acceptor enthalpies provide a scale of solid acidity that is temperature independent from room temperature up to temperatures where acid catalysts are commonly used (200–300 °C).

A fundamental scale of acidity of solids will require a definition of the reaction involved. Solution acid-base equilibria which are well understood, invariably involve displacement reactions. Even in alkane solvents, solvent molecules undergoing dispersion interactions with the acid and base are displaced when the donor coordinates to the acid. Earlier results from this laboratory<sup>11</sup> have shown that in poorly solvating solvents the product and reactant nonspecific dispersion interactions cancel and do not contribute to enthalpies measured in solution. In contrast gas phase donor-acceptor interactions, e.g., proton and cation affinities, are not displacement reactions and have dispersion as well as donor-acceptor contributions to the measured enthalpies. In contrast to solution enthalpies, that are fit to a two term electrostatic-covalent model, the

\* Corresponding author. Tel.: (352) 392-6043. Fax: (352) 392-4658.

† Departamento de Química – Universidade de Brasília, Brasília-DF, 70919-910, Brazil.

‡ Intevep S. A. Research and Technological Center of Petróleos de Venezuela.

⊗ Abstract published in *Advance ACS Abstracts*, May 1, 1997.

- (1) Corma, A. *Chem. Rev.* **1995**, *95*, 559.
- (2) Vaughan, D. E. W. *Properties and Applications of Zeolites*; Townsend, R. P. Ed.; Soc. Chem. Ind.: London, 1980; p 294.
- (3) Flaningan, E. M. *Zeolites: Sciences and Technology*; NATO ASI, Series E80, Ribeiro, F. R., et al., Eds.; 1984; p 3.
- (4) (a) Guisnet, M. R. *Acc. Chem. Res.* **1990**, *23*, 392. (b) Carniti, P.; Gervasini, A.; Auroux, A. *J. Catal.* **1994**, *150*, 274.
- (5) Farcasiu, D.; Ghenciu, A.; Li, J. Q. *J. Catal.* **1996**, *158*, 116.
- (6) (a) Srinivasan, R.; Keogh, R. A.; Ghenciu, A.; Farcasiu, D.; Davis, B. H. *J. Catal.* **1996**, *158*, 502. (b) Wan, K. T.; Khouw, C. B.; Davis, M. E. *J. Catal.* **1996**, *158*, 311. (c) Farneth, W. E.; Gorte, R. J. *Chem. Rev.* **1995**, *95*, 615.
- (7) (a) Cardona-Martinez, N.; Dumesic, J. A. *Adv. Catal.* **1992**, *38*, 149. (b) Yaluri, G.; Larson, R. B.; Kobe, J. M.; Gonzalez, M. R.; Fogash, K. B.; Dumesic, J. A. *J. Catal.* **1996**, *158*, 336. (c) Chen, D. T.; Sharma, S. B.; Filimonov, I.; Dumesic, J. A. *Catal. Lett.* **1992**, *12*, 201.
- (8) (a) Parrillo, D. J.; Lee, C. J.; Gorte, R. J. *Appl. Catal. A* **1994**, *110*, 67. (b) Farneth, W. E.; Gorte, R. J.; Parrillo, D. J. *J. Am. Chem. Soc.* **1993**, *115*, 12441. (c) Biaglow, A. I.; Gorte, R. J.; Kokotailo, G. T.; White, D. J. *J. Catal.* **1994**, *148*, 779. (d) Lee, C.; Parrillo, D. J.; Gorte, R. J.; Farneth, W. E. *J. Am. Chem. Soc.* **1996**, *118*, 3262.
- (9) Healy, M. H.; Wieserman, L. F.; Arnett, E. M.; Wefers, K. *Langmuir* **1989**, *5*, 114.

(10) (a) Lim, Y. Y.; Drago, R. S.; Babich, M. W.; Wong, N.; Doan, P. E. *J. Am. Chem. Soc.* **1987**, *109*, 169. (b) Chronister, C. W.; Drago, R. S. *J. Am. Chem. Soc.* **1993**, *115*, 793.

(11) (a) Nozari, M. S.; Drago, R. S. *Inorg. Chem.* **1972**, *11*, 280. (b) Nozari, M. S.; Drago, R. S. *J. Am. Chem. Soc.* **1972**, *94*, 6877. (c) Drago, R. S.; Cundari, T. R.; Ferris, D. C. *J. Org. Chem.* **1989**, *54*, 1042. (d) Drago, R. S.; Ferris, D. C.; Wong, N. *J. Am. Chem. Soc.* **1990**, *112*, 8953.

quantitative correlation of gas phase ion–molecule reactions requires<sup>11c,d</sup> a transfer term to accommodate the electron transfer and dispersion components that are minor in solution displacement reactions. This transfer term is appreciable even for the proton affinity of argon ( $E_B = C_B = 0$  for argon) in which case the transfer contribution is mainly a dispersion interaction. The very large dispersion and transfer terms make the proton a very poor model for condensed phase reactions and account in part for the poor correlation  $R^2 = 0.79$  when gas–solid enthalpies of reactions of zeolites with substituted pyridines and amines<sup>8</sup> are plotted vs proton affinities.

As a result of the above considerations, reactions of solid acids with bases in poorly solvating solvents will not produce the same enthalpy as measured in gas phase–solid reactions but can provide complimentary information with differences providing an estimate of the gas–solid dispersion component. One can argue that solution enthalpies devoid of dispersion contributions provide a better scale of acidity for solids. Even a gas phase, solid acid catalyzed reaction is a displacement reaction in which products are displaced by reactants. The dispersion component is partially cancelled and donor–acceptor contributions dominate substrate binding. Furthermore, as manifested in spectral shifts, strong donor–acceptor interactions make much larger perturbations in the electronic structure of a molecule than dispersion interactions.<sup>12</sup> Acid catalysis occurs because of the changes induced in the electronic structure of the coordinated molecule. Clearly understanding differences in the reactivity of zeolites will require understanding differences in their donor–acceptor strengths.

This article will present the results from cal-ad studies aimed at measuring the acidity of HZSM-5. Studies with pyridine, 2,6-lutidine, and 2,6-di-*tert*-butylpyridine provide a unique thermodynamic characterization of the acid sites and their distribution in the solid. The factors that lead to an incorrect assessment of the acidity and number of strong acid sites with gas–solid calorimetry, TPD, and isopropyl amine decomposition are discussed.

## Experimental Section

**Materials.** HZSM-5 (Lot No. 91101036K), from the PQ corporation, with an advertised Si/Al ratio of 30, 0.05% Na<sub>2</sub>O, and surface area of 430 m<sup>2</sup>/g was used. Our atomic absorption measurements indicated that the bulk Si/Al ratio was 36. Infrared, calorimetric, and adsorption studies were carried out on samples that were dried under flowing oxygen for 2 h at 450 °C and then evacuated at 450 °C overnight. The oxygen flow was used to assure that no organic material was present in the samples. Elemental analysis was performed by the Microanalysis Laboratory at the University of Florida and carbon as well as nitrogen were absent on the original and calcined samples. The drying apparatus was filled with argon and transferred to a drybox to load the calorimetric cell.

Pyridine (Fisher) was distilled over CaH<sub>2</sub> using a 12 in. Vigreux column. 2,6-Di-*tert*-butylpyridine and 2,6-lutidine (Aldrich, 97%) were used as supplied. Hexane (Aldrich, 99%) was distilled over P<sub>2</sub>O<sub>5</sub> and stored over 4Å molecular sieves.

**Calorimetric Measurements.** One gram samples of HZSM-5 were slurried in 100 mL of hexane and reacted with pyridine, 2,6-lutidine, or 2,6-di-*tert*-butylpyridine solutions in hexane. Addition of pyridine solutions to the calorimeter was made using a 2.5 mL Hamilton gas-tight syringe with calibrated stops. The heat evolved was measured after each injection. The calorimetric is a 150 mL silvered dewar flask equipped with a heater coil and thermistor. The thermistor is calibrated prior to each calorimetric experiment. Repeat calorimetric runs give an average deviation of 0.005 calories.

**Adsorption Measurements.** Adsorption experiments were carried out using approximately 1 g of HZSM-5 in a sealed round bottom flask containing 100 mL of hexane. After each injection, at least 3 min were allowed for equilibrium to be reached. Then a 1 mL sample is removed from the flask and placed into a quartz 1 cm UV–vis cell. One milliliter of solvent is added back into the flask to maintain a constant volume. The absorbance of pyridine at 251 nm, 2,6-di-*tert*-butylpyridine at 258 nm, and 2,6-lutidine at 265 nm are measured with a Perkin Elmer Lambda 6 UV/vis spectrophotometer, and these absorbances are used to calculate the concentrations of pyridine, 2,6-lutidine, and 2,6-di-*tert*-butylpyridine in solution at equilibrium. By knowing the amount in solution at equilibrium and the amount added, the amount absorbed by the solid is given by the difference. Since one is combining raw data from calorimetric and adsorption measurements in the data analysis, it is essential in the cal-ad procedure to use the same ratio of solid to solution in both measurements. Repeat titrations give absorbance values with an average deviation of 0.003 absorbance units.

**Cal-Ad Analysis.** It is important that the concentration of base and the ratio  $V/g$  where,  $V$  is the volume of solution (liter) and  $g$  is the mass of solid (grams), be the same in both the calorimetric and adsorption experiments. Since we need to resolve sites 1 and 2 contributions to  $-\Delta H_{AVE}$ , it is important to use very dilute solutions of pyridine in the titration. It is also important to add eventually a total amount of pyridine that will saturate at least 60% of site 2. Since porosity can lead to a large  $K$  for binding even when  $-\Delta H$  is small, the usual cal-ad procedure of fitting the adsorption data first to generate concentrations of base in solution for the subsequent fit of the heat evolved cannot be used. In the case of HZSM-5, for example, detectable amounts of pyridine are not seen in solution until 0.1 mmol of pyridine has been added (point 7 of increasing concentration in Figure 3). Accordingly, the data workup differs slightly from that reported for silica gel.<sup>10b</sup> Entering the equilibrium concentration of pyridine in solution calculated from the adsorption experiment into the calorimetric expression, rough estimates of  $n$ 's and  $K$ 's are obtained for sites 1 and 2. The following equation is used to produce these first estimates:

$$\frac{h}{g} = \sum \frac{n_i K_i [B]}{1 + K_i [B]} \Delta H_i$$

where  $h$ , the sum of heat evolved from calorimetric experiment  $= \Sigma -([T] - [B])v\Delta H_i$ ;  $\Delta H_i$  is the enthalpy for binding to each site;  $[T]$  is the total concentration of base added (mol/L) in each injection from the calorimetric experiment; and  $[B]$  is the equilibrium concentration of base in solution.

The resulting  $K$ 's and  $n$ 's are used to generate an adsorption isotherm from which the equilibrium concentrations of base in those solutions that are too small to measure are calculated for each point in the adsorption curve. Rather than graphically interpolate the adsorption isotherm to obtain these concentrations, the isotherm is fit to a polynomial series.

For one site the following series is used

$$(v/g)[T] = x^2[B]^2 + x[B]$$

where  $v/g$  = volume (liters)/mass of solid (grams);  $[T]$  is the total concentration of base added (mol/L) for each injection in the calorimetric experiment;  $[B]$  is the equilibrium concentration of base in solution;  $x^2 = v/gK_1$  and  $x = n_1K_1 - v/gK_1[T] + v/g$ .

For two sites the following series is used

$$(v/g)[T] = x^3[B]^3 + x^2[B]^2 + x[B]$$

where

$$x^3 = K_1K_2v/g; \quad x^2 = n_1K_1K_2 + n_2K_1K_2 - v/gK_1K_2[T] + v/gK_1 + v/gK_2; \quad \text{and } x = n_1K_1 + n_2K_2 - v/gK_1[T] - v/gK_2[T] + v/g$$

These concentrations are then used as the experimental base concentrations in solution for the adsorption isotherm for those solutions too dilute to measure, and the combined adsorption and calorimetric data are solved for the best fit  $n$ 's and  $K$ 's. These  $n$ 's and  $K$ 's are then

(12) Drago, R. S. *Applications of Electrostatic-Covalent Models in Chemistry*; Surfside Scientific Publishers: Gainesville, FL, 1994.

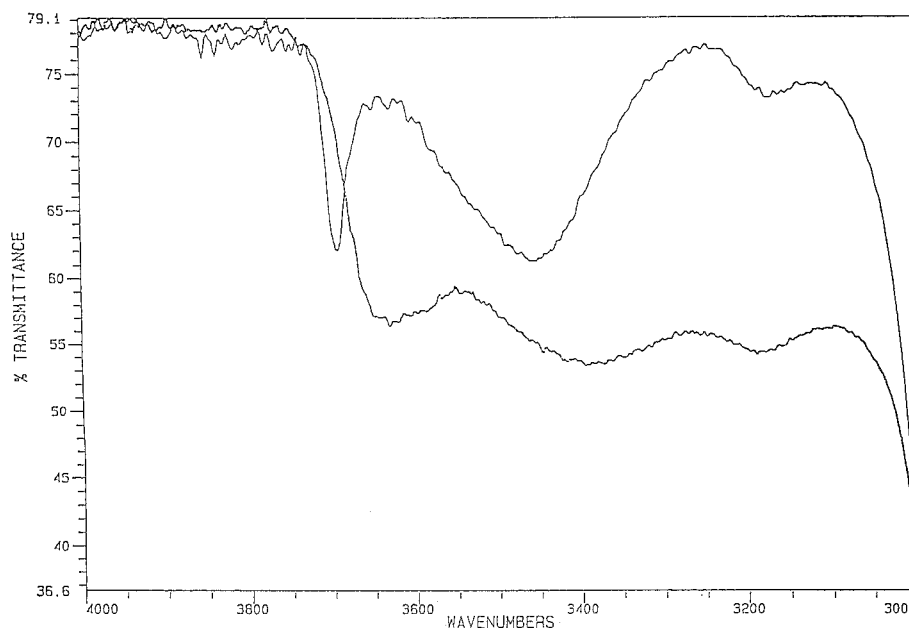


**Figure 1.** FTIR spectra in Nujol mulls of H2SM-5 as received and after drying at 450 °C in vacuum.

used in the above expressions to recalculate the concentrations of base in solution for those systems too dilute to measure as described above and the combined adsorption and calorimetric data refit. This procedure is repeated until the  $K$ 's and  $n$ 's converge. This procedure differs from that utilized for silica gel and is recommended for porous solids that have such large affinities for adsorbates that solution concentrations cannot be determined even when  $-\Delta H$  is small.

**Infrared Measurements.** All IR spectra were recorded as Nujol mulls on sodium chloride plates, using a Nicolet 5DXB FTIR spectrophotometer.

**Solid-State NMR.** Solid-state  $^1\text{H}$ ,  $^{27}\text{Al}$ , and  $^{29}\text{Si}$  NMR spectra were recorded under magic angle spinning (MAS) at room temperature on a Bruker MSL-300 spectrometer at 300.13, 78.15, and 59.62 MHz, respectively. The rotors were driven by dry air, and the magic angle was set precisely by observing the  $^{79}\text{Br}$  resonance of KBr. All the spectra were recorded with a 4 mm MAS probe.

Prior to  $^1\text{H}$  MAS NMR experiments, the sample was dehydrated in 10 mm o.d. glass tube for 6 h at 673 K under vacuum (pressure of  $10^{-5}$  mbar) and transferred under controlled atmosphere into the rotor. No rehydration occurred during the experiments as shown by  $^1\text{H}$  NMR. The spectrum was recorded following an echo sequence ( $\pi/2$ - $\tau$ - $\pi$ ) where the echo time  $\tau$  is equal to the inverse of the spin rate,  $\pi/2$  is  $5 \mu\text{s}$ , and the pulse delay is fixed to 30 s (full relaxation). The chemical shift is referenced to external tetramethylsilane. The rotor was spun at a rotation frequency of 10 KHz. For  $^{29}\text{Si}$ , one pulse sequence with a  $\pi/2$  pulse of  $5 \mu\text{s}$  was used. The cycle time of 60 s gives complete relaxation of the spins of the silicon species. The  $^{27}\text{Al}$  spectrum was recorded using a one pulse sequence with a  $\pi/8$  pulse, i.e.,  $0.6 \mu\text{s}$  and high power proton decoupling. A  $\pi/2$ ,  $5 \mu\text{s}$  pulse was used for the liquid reference. The rotors were spun at 10 KHz. The shifts are referenced to external TMS and aqueous hexaquo aluminum nitrate, respectively.

The amount of each silicon environment per unit cell can be calculated with the following equations<sup>13</sup>

$$[\text{Si}/\text{Al}]_{\text{Framework}} = \frac{\sum_{i=0}^4 \text{Si}(n\text{Al})}{0.25 \sum_{i=0}^4 n\text{Si}(n\text{Al})} = \frac{\text{Si}(1\text{Al}) + \text{Si}(0\text{Al},\text{OH}) + \text{Si}(0\text{Al})}{0.25\text{Si}(1\text{Al})}$$

The last term results because only  $n = 0$  and  $n = 1$  species are present at this low aluminum content.

The spectra were deconvoluted using the WINFIT 950425 program from Bruker GMBH.

## Results and Discussion

In view of confusing terminology in the zeolite literature it is important to define the terms used in the donor-acceptor literature and in this article. The term Lewis acid will be reserved to distinguish aluminum or silicon atom acceptor centers. There is no evidence for this type of site in HZSM-5 from our work. The terms Brönsted site and hydrogen bond site are used to distinguish the products of a reaction. Any protonic site is a *potential Brönsted site* if a strong enough base is employed. A site that hydrogen bonds to pyridine without proton transfer will not transfer the proton to most neutral organic bases and will be called a hydrogen bond site. Sites that proton transfer to pyridine will be called a Brönsted site but could function as a strong hydrogen bond site toward a weak donor.

**Infrared and NMR Studies of HZSM-5.** HZSM-5 was chosen as the first zeolite to be studied by cal-ad in view of the extensive characterization reported for this material. Zeolites have high affinity for water, and precautions must be taken to dry the samples well and to exclude water during the measurements. Figure 1 shows the infrared spectra in the hydroxyl region of the sample as received and that after drying for 24 hours at 450 °C under vacuum with periodic flushing of the apparatus with argon. After drying, two bands remain: a sharp one at  $3694 \text{ cm}^{-1}$  and a broad band at  $3457 \text{ cm}^{-1}$ . The latter is attributed to the bridging  $\text{Al}-(\text{OH})-\text{Si}$  sites and the former to the nested silanols needed for charge compensation at a cation vacancy.<sup>14</sup> When the sample is deuterated and dried,<sup>14b</sup> these two bands shift to 2750 and  $2650 \text{ cm}^{-1}$ . When this sample is titrated with pyridine in a calorimetric run, the spectrum of the remaining sample shows no adsorption in this region but has three bands in the pyridine region from 1624 to  $1450 \text{ cm}^{-1}$  that have been assigned to either Brönsted (pyridinium at 1543 and  $1491 \text{ cm}^{-1}$ ) or hydrogen bond sites (pyridine adducts at  $1624 \text{ cm}^{-1}$ ). The absence of vibrations in the OH stretch region indicate water has been completely removed for a pyridine- $\text{H}_2\text{O}$  adduct would absorb in this region. The solid-state NMR in Figure 2 (*vide infra*) also confirms the absence of water.<sup>13</sup> All reported calorimetric results are for dried samples of HZSM-5 that were checked by infrared to ascertain the absence

of water. In view of the difficulties associated with obtaining information about acidity from the fine structure of infrared OH bands<sup>15,16</sup> no further analysis of the infrared spectra were undertaken.

#### Shortcomings in Average Enthalpies from Calorimetry.

Cal-ad results for HZSM-5, particularly the amount of sites, are expected to be sample dependent. Thus it is important to emphasize that the results reported here are for a sample with a bulk Si/Al ratio of 36 and with the spectral features described above and in the NMR section. A material used commercially in catalytic reactions is selected for study. The base pyridine is selected as the donor in order to avoid the amphoteric interaction encountered when protonic donors (e.g., NH<sub>3</sub>) are studied. When NH<sub>3</sub>, RNH<sub>2</sub>, and R<sub>2</sub>NH are employed,<sup>7,8</sup> electron pair donation by the donor makes the N-H proton more acidic which can lead to increased hydrogen bonding of this N-H proton to the framework. This secondary hydrogen bonding by the N-H proton is analogous to the interactions of zeolites with water.<sup>15b</sup> Upon coordination of water to the Brønsted or hydrogen bond site of the zeolite, a secondary hydrogen bonding interaction of a water O-H to the oxygen of an Si-O-Si group occurs. With protonic bases, amphoteric hydrogen bonding interactions would give added contributions to the measured enthalpies and distort the solid acidity data.

The adsorption measurements of pyridine by HZSM-5 are shown in Figure 3 where the mmol of pyridine adsorbed by 1 g of the solid slurried in 100 mL of hexane are plotted vs the amount of pyridine in solution. The  $h'$  axis of Figure 3 is a plot of the heat evolved when pyridine is added to 1 g of HZSM-5 slurried in 100 mL of hexane.

Figure 4 is a plot of the average enthalpy of reaction calculated for those base additions in which 95% of the added pyridine is adsorbed by the solid. Average data from the three titrations with 0.1 M pyridine solutions are shown. The average enthalpy is calculated using a limiting reagent assumption by dividing  $h'$  by the moles of pyridine added and as such is an average of the sites that react with each incremental addition of pyridine. This average enthalpy curve is easily calculated, but it measures the enthalpy and amounts of the strongest sites only when a single type of site exists or when the equilibrium constants for different sites are significantly different ( $\sim 10^3$ ). Since nearly all the pyridine is adsorbed even for those points where the  $-\Delta H_{AVE}$  has decreased by a considerable amount,  $K_1$  and  $K_2$  are both large. The gradual decrease in  $-\Delta H_{AVE}$ , in contrast to a sharp break, indicates that the second site begins to react before the first site is completely reacted. The  $-\Delta H_{AVE}$  decreases as weaker sites make a larger contribution to the average enthalpy. The essential question is as follows: are there contributions to the  $-\Delta H_{AVE}$  calculated for the first three base additions from a weaker site. This would make the enthalpy of site 1 larger than that given by  $-\Delta H_{AVE}$  from the initial base additions. This question cannot be answered using only calorimetric data and introduces uncertainty in acidities reported in all the calorimetric literature studies<sup>7-9</sup> that calculate an

(13) (a) Batamack, P.; Doremieux-Morin, C.; Fraissard, J.; Freude, D. *J. Phys. Chem.* **1991**, *95*, 3790. (b) Klinowski, J. *Colloids Surfaces* **1989**, *36*, 133.

(14) (a) Jacobs, P. A.; von Ballmoos, R. *J. Phys. Chem.* **1982**, *86*, 3050. (b) Farneth, W. E.; Roe, D. C.; Kofke, T. J. G.; Tabak, C. J.; Gorte, R. J. *Langmuir* **1988**, *4*, 152.

(15) (a) Sauer, J. *Science* **1996**, *271*, 774. (b) Smith, L.; Cheetham, A. K.; Morris, R. E.; Marchese, L.; Thomas, J. M.; Wright, P. A.; Chen, J. *Science* **1996**, *271*, 799.

(16) (a) Brand, H. V.; Curtiss, L. A.; Iton, L. E. *J. Phys. Chem.* **1992**, *96*, 7725. (b) Schroder, K. P.; Sauer, J.; Leslie, M.; Catlow, C. R. A.; Thomas, J. M. *Chem. Phys. Lett.* **1992**, *188*, 320.

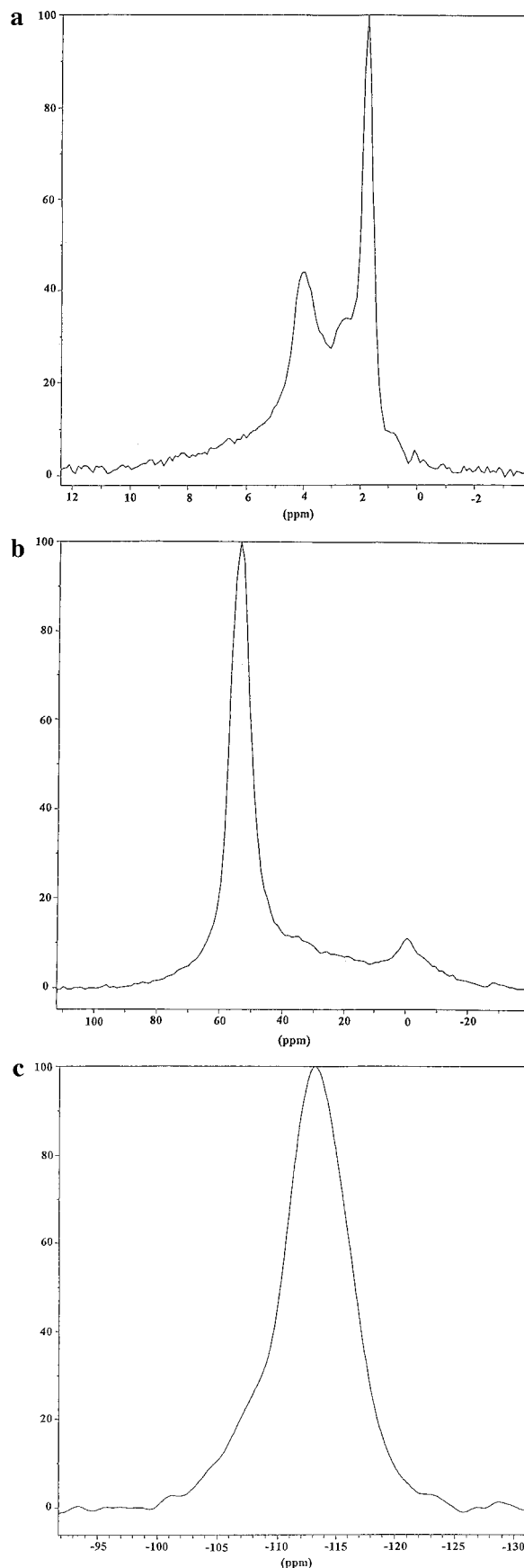


**Figure 2.** <sup>1</sup>H (a), <sup>27</sup>Al (b), and <sup>29</sup>Si (c) NMR spectra of solid HZSM-5.

enthalpy for a solid with multiple acid sites using the limiting reagent assumption.

The potential severity of the limiting reagent problem is illustrated with the data in Table 2. The table presents the moles

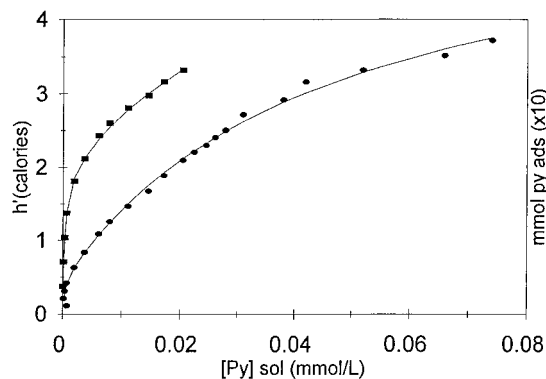


**Figure 3.** Adsorption isotherm and heat of adsorption versus concentration of pyridine in solution: (■) calorimetric data points, (●) adsorption data points, and (—) solid line: calculated using values from Table 1.

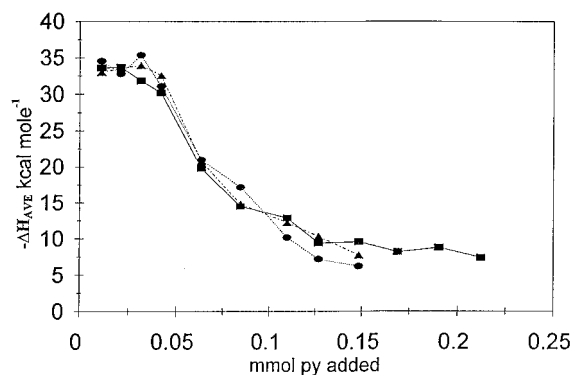


**Figure 4.** Average enthalpies of reaction versus mmol of pyridine added.

of base adsorbed on two sites for various  $K_2$  and  $n_2$  values when  $K_1$  and  $n_1$  is that from cal-ad for our HZSM-5 sample; *i.e.*, a  $K_1$  value of  $2 \times 10^6$  L/mol and an  $n_1$  of 0.06 mmol. The data are presented for the very low equilibrium base concentrations in solution that correspond to the first four base additions of the titration in Figure 3. For case I, when  $K_2$  is  $1 \times 10^4$  and  $n_2$  is 0.6, the first base addition (0.01 mmol/g) involves reaction of 6% of site 2 and 94% of site 1. By the fourth base addition, corresponding to 0.04 total mmol of pyridine adsorbed per gram of zeolite, there is only  $8.7 \times 10^{-7}$  mol/L of pyridine in solution, and the values calculated for sites 1 and 2 show that 13% of the total base added coordinates to site 2. For the case in column II where  $K_1$ ,  $n_1$ , and  $K_2$  are the same as in case I, but  $n_2$  is increased to 1.0 mmol  $g^{-1}$ , the percent of added base coordinated to site 2 in the first base additions increases from 6% to 11% and from 13% to 24% for the fourth base addition. Increasing  $n_2$  to 2.0 (column III) results in 20% of the added base coordinating to site 2 for the first base addition and 45% coordinating to site 2 for the fourth addition. Values for other  $K$ 's and  $n$ 's are given in Table 2.

Clearly, one cannot compare the acidity of solid zeolites using an average enthalpy from a limiting reagent assumption unless  $K_1$  is three orders of magnitude larger than  $K_2$  and  $n_2$  is less than an order of magnitude larger than  $n_1$ . Since this information is not known, a priori, the  $K$ 's and  $n$ 's from gas phase calorimetric studies reported to date cannot be trusted as a measure of strongest site strength.

**Cal-Ad Results.** In contrast to studies based on the limiting reagent assumption, the cal-ad procedure simultaneously solves calorimetric and adsorption data (Figure 3) to produce individual  $K$ 's,  $-\Delta H$ 's, and  $n$ 's for all the sites reacting with the base. The solvent *n*-hexane was selected because it has a kinetic

diameter around 4.3 Å.<sup>17</sup> Since the experimental data over the concentration range employed is fit to within experimental error of the measurement using a two-site model, the number of sites is discriminated. The resulting thermodynamic values are given in Table 1. The accuracy of the site 1 equilibrium constants and entropies may be less than their precisions because nearly complete adsorption of base occurs up to the saturation point. The main conclusions will be drawn from enthalpies. The enthalpies of donor–acceptor binding are  $-42.1 \pm 0.8$  and  $-8.6 \pm 3.8$  kcal mol<sup>-1</sup> for the two sites. Our studies extend up to 0.4 mmol of pyridine added for 0.6 mmol of total acid sites. Higher concentrations would improve the error limits of the site 2 parameters and might reveal that site 2 consists of two sites. However, our main concern is with site 1 parameters, and these are defined well enough to produce accurate enthalpy values for and quantities of the strongest site.

Comparison of the enthalpy of interaction of pyridine for the first site with the enthalpy of reaction of pyridine with SGAlCl<sub>2</sub> ( $-51$  kcal mol<sup>-1</sup>) shows that HZSM-5 is not a superacid but is a considerably stronger acid than the strongest sites on silica gel ( $-12$  kcal mol<sup>-1</sup>) or  $\gamma$ -alumina ( $\sim -18$  kcal mol<sup>-1</sup>). The thermodynamic data for the second site on HZSM-5 is comparable to that of the sites on silica gel. The equilibrium constants for pyridine reacting with silica gel and the second site of HZSM-5 are also of the same order of magnitude. In silica gel these are not Brønsted sites toward pyridine. The infrared of adsorbed pyridine on silica gel indicates that the  $-12$  kcal mol<sup>-1</sup> sites correspond to silanol hydrogen bonding sites ambiguously referred to as Lewis sites in the literature. Thus, site 2 in HZSM-5 is a hydrogen bonding site arising from bridging Al(OH)Si and SiOH functionality. The observation of a Brønsted peak in the infrared for adsorbed pyridine is attributed to site 1.

HZSM-5 contains 12 inequivalent T-sites. The excellent fit of the experimental data at low base concentration to this two site model indicates that the strong acid sites and the hydrogen bonding sites are homogeneous groups within the experimental resolution of our measurements ( $\sim 2$  kcal mol<sup>-1</sup>). It is not possible to determine which of the different crystallographic sites in HZSM-5 have comparable acidities and are contained in the  $K_1$  and  $n_1$  values. Titrations with other bases and <sup>1</sup>H, <sup>29</sup>Si, and <sup>27</sup>Al NMR provide more information on this point (*vide infra*).

The line connecting the experimental  $h'$  values in Figure 5 gives the sum of heat evolved for incremental additions of pyridine to 1 g of HZSM-5 in hexane. Using the data in Table 1, the experimental curve can be decomposed into the two contributions from sites 1 and 2. Site 1 (dashed line) reacts to completion in the titration. The second site (bold line) does not react completely. The contribution of the second site to all measured  $h'$  values, as calculated in Table 2, can be seen in this plot.

Figure 6 shows a similar plot of the contributions of the two sites to the adsorption data. The complete coordination of the strongest site is again seen (dashed line). Even though the adsorption data was measured in concentrated pyridine solution, the second site is still incompletely coordinated by pyridine. Considering the error in  $n_2$ , 60–75% of the second site has reacted at the highest concentration used.

**Strong Acid Site Location.** Cal-ad studies of the bases 2,6-di-*tert*-butylpyridine and 2,6-lutidine were also carried out. These were selected because the former is too large to enter into the pores of HZSM-5, and access to the pores by the latter

(17) Derouane, E. G. *Zeolite: Science and Technology*; NATO ASI Series, Ribeiro, F. R., et al., Eds.; 1984, 347.

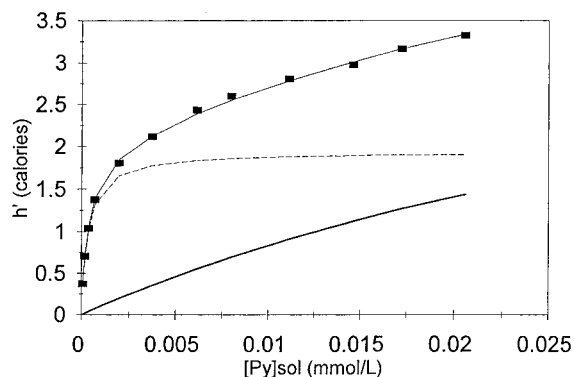
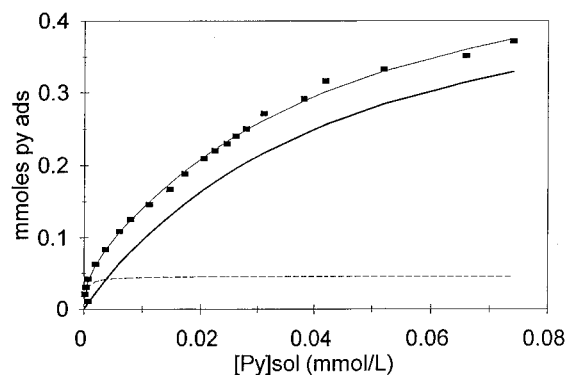
**Table 1.** Thermodynamic Parameters Obtained in Hexane Solvent for Reactions of HZSM-5 (Bulk Si/Al of 36) with Pyridine, 2,6-Lutidine, and 2,6-Di-*tert*-butylpyridine

	pyridine	2,6-lutidine	2,6-di- <i>tert</i> -butylpyridine
$n_1$ (mmol/g)	$0.0415 \pm 0.0057$	$0.0529 \pm 0.0074$	$0.0342 \pm 0.0007$
$K_1^{298}$ ( $M^{-1}$ )	$4.9 \times 10^6 \pm 2.3 \times 10^6$	$7.4 \times 10^5 \pm 2.6 \times 10^5$	$6.9 \times 10^4 \pm 1.0 \times 10^4$
$-\Delta H_1$ (kcal/mol)	$42.1 \pm 0.8$	$19.0 \pm 0.3$	$10.9 \pm 0.1$
$-\Delta G_1^{298}$ (kcal/mol)	9.12	8.00	6.59
$\Delta S_1$ (cal/deg)	-111	-37	-14
$n_2$ (mmol/g)	$0.53 \pm 0.01$	$0.13 \pm 0.06$	
$K_2^{298}$ ( $M^{-1}$ )	$2.3 \times 10^4 \pm 2.0 \times 10^3$	$8.8 \times 10^3 \pm 2.3 \times 10^3$	
$-\Delta H_2$ (kcal/mol)	$8.6 \pm 3.8$	$5.4 \pm 1.7$	
$-\Delta G_2^{298}$ (kcal/mol)	5.95	5.38	
$\Delta S_2$ (cal/deg)	-9	-0.1	

**Table 2.** Moles Adsorbed at Two Competing Sites as a Function of  $K$  and  $n$ 

base solution [M] ( $\times 10^7$ )	moles ads <sup>a</sup> site 1 ( $\times 10^3$ )	moles ads site 2 ( $\times 10^3$ )				
		I <sup>b</sup>	II <sup>c</sup>	III <sup>d</sup>	IV <sup>e</sup>	V <sup>f</sup>
1.17	0.0114	0.0007	0.0012	0.0023	0.0002	0.007
2.67	0.0209	0.0016	0.0027	0.0053	0.0005	0.016
5.01	0.0300	0.003	0.005	0.010	0.001	0.029
8.70	0.0381	0.005	0.009	0.017	0.002	0.048

<sup>a</sup>  $K_1 = 2 \times 10^6$  L/mol;  $n_1 = 6 \times 10^{-5}$  mol/g. <sup>b</sup>  $K_2 = 1 \times 10^4$  L/mol;  $n_2 = 6 \times 10^{-4}$  mol/g. <sup>c</sup>  $K_2 = 1 \times 10^4$  L/mol;  $n_2 = 1 \times 10^{-3}$  mol/g. <sup>d</sup>  $K_2 = 1 \times 10^4$  L/mol;  $n_2 = 2 \times 10^{-3}$  mol/g. <sup>e</sup>  $K_2 = 1 \times 10^3$  L/mol;  $n_2 = 2 \times 10^{-3}$  mol/g. <sup>f</sup>  $K_2 = 1 \times 10^5$  L/mol;  $n_2 = 6 \times 10^{-4}$  mol/g.

**Figure 5.** Sum of heat evolved versus concentration of pyridine in solution for two acid sites: (■) calorimetric data points, (- -) dashed line: process 1 (first site), (■) bold line: process 2 (second site), and (■) solid line: calculated using values from Table 1.**Figure 6.** Adsorption isotherm versus concentration of pyridine in solution: (■) adsorption data points, (-) solid line: calculated using values from Table 1, (- -) dashed line: process 1 (first site), and (—) bold line: process 2 (second site).

is expected to be limited. HZSM-5 is known to have two intersecting channel systems: one is straight and the other is sinusoidal and perpendicular to the former. Both channel systems have 10-membered-ring, elliptical openings with a 5.5 Å internal diameter. Saito and Foley<sup>18</sup> report two steps in the adsorption isotherms of high Si/Al ratio zeolites. The first peak

in a pore size analysis corresponds to adsorption in pores of 5.5 Å diameter. The second peak, corresponding to a 7.7 Å diameter, does not correspond to a structural feature of the zeolite and is reported to be a nonphysical result.

Since 2,6-di-*tert*-butylpyridine cannot enter into the channels of HZSM-5, this titration gives information about the acidity of the external solid surface. The experimental data are fit to within experimental error of the measurement using a one-site model giving the values in Table 1. A considerably smaller enthalpy of  $-10.9 \pm 0.2$  kcal mol<sup>-1</sup> results compared to  $-42.1$  kcal mol<sup>-1</sup> for pyridine. No strong acid sites are located on the exterior surface of the zeolite. The small  $n_1$  value from this titration shows that the surface contains about 6% of the weak  $n_2$  type sites found for pyridine reacting with HZSM-5 with 94% of the acid sites being located in the channels.

The reaction of HZSM-5 with 2,6-lutidine produces a very interesting result. An enthalpy of  $-19 \pm 0.3$  kcal mol<sup>-1</sup> is obtained for the first site, and an enthalpy of  $-5.4 \pm 1.7$  kcal mol<sup>-1</sup> is obtained for the second site. Site 1 for the donor 2,6-lutidine is not accessing the strong site 1 of pyridine. The low enthalpy for site 1 with 2,6-lutidine indicates that the strongest sites for this base are hydrogen bond sites. These enthalpies suggest site 2 for pyridine has large error limits, because it contains the two sites detected with 2,6-lutidine.

The  $n$ -values are very informative. They suggest that the strongest sites for pyridine ( $-42$  kcal mol<sup>-1</sup>) and 66% of site 2 for pyridine are not accessed by 2,6-lutidine. Comparing  $n_1$  for 2,6-lutidine and 2,6-di-*tert*-butylpyridine indicates that there are 0.15 mmol/g of hydrogen bond sites accessed by the former in addition to the 0.03 mmol/g of surface sites. The second site for 2,6-lutidine like that for pyridine is very weak and could involve hydrogen bonding to isolated silanols at locations not accessed by 2,6-di-*tert*-butylpyridine. Many of these sites are accessed by pyridine ( $n_2 = 0.53$ ) and not by 2,6-lutidine ( $n_1 + n_2 = 0.18$ ). The lutidine site 1 is tentatively assigned to arise from the group of sites included in site 2 for pyridine. Studies at much higher concentrations of pyridine than those used in this titration are needed to discriminate the pyridine site 2 components.

The results from this study indicate a limited access strong site, I, limited access hydrogen bonding sites, II, interior hydrogen bonding sites III, and surface sites IV. Two types of intersecting channels exist in HZSM-5, one is straight and the other zig-zag. The latter contains crevasses and curves that could contain the limited access strong Brønsted sites (I) and the hydrogen bond sites that cannot be accessed by 2,6-lutidine (II). The entropy for site 1 bonding to pyridine would suggest organization of the solid to accommodate the conjugate base.

**Comparison of Cal-Ad with Other Acidity Measures.** Much has been published on the acidity of HZSM-5 often leading to apparently conflicting conclusions which differ from

those given above. In this section, we shall reinterpret results from reported indirect measures of zeolite acidity in order to show that the cal-ad measure of  $K$ ,  $n$ , and  $-\Delta H$  is not inconsistent with any of these experimental observations.

HZSM-5 has been extensively studied by gas–solid calorimetry. At the elevated temperatures ( $\sim 200$  °C) used in gas–solid microcalorimetry, the larger  $-\Delta H$  and negative entropy change expected for site 1 than 2 lead to values of  $K_1$  and  $K_2$  that are much closer than those at room temperature. This leads to the expectation of simultaneous reaction of both sites of HZSM-5 with pyridine in the gas phase calorimetric titration producing a constant  $-\Delta H$  of 48 kcal mol<sup>-1</sup> for up to 0.6 mmol of added pyridine. The 0.6 mmol correspond to the sum of  $n_1$  and  $n_2$  from the solution analysis supporting the prediction that the  $K$ 's would be close and that both sites would react simultaneously producing an average enthalpy.

The larger  $-\Delta H_{\text{AVE}}$  from the gas phase study compared to the cal-ad average is due to contributions from the dispersion component in addition to the donor–acceptor component to both sites 1 and 2 in the gas phase calorimetric study. Estimating the total gas phase enthalpies for site 1 and 2 at  $-75$  and  $-43$  kcal mol<sup>-1</sup> for the purpose of illustration, a set of  $K$ 's and  $n$ 's could be found that after the first base addition caused reaction of site 1 and site 2 to occur in a ratio of 1:5 up to the 0.6 mmol of base added. This would give a nearly constant  $-\Delta H$  of 48 kcal mol<sup>-1</sup> until site 1 was consumed. As more base is added the average enthalpy would then be dominated by the equilibrium involving site 2 until it is consumed. The purpose in proposing this scenario is to demonstrate that this or other combinations of  $-\Delta H$ 's,  $n$ 's, and  $K$ 's cannot be eliminated when only calorimetry data is available. The results are ambiguous unless accompanied by a determination of  $K$ .

It would be of interest to factor out the dispersion and donor–acceptor components from gas phase calorimetric studies. Unfortunately the reported gas phase values are some weighted average of sites 1 and sites 2. Temperature dependent studies<sup>19</sup> of the adsorption of gaseous propane by HZSM-5 give an enthalpy of  $-9.6$  kcal mol<sup>-1</sup>. Using a reported correlation,<sup>19</sup> a value of about  $-22$  kcal mol<sup>-1</sup> is estimated for hexane using the van der Waals constant<sup>19</sup> and a similar value is expected for pyridine. This dispersion component combined with the donor–acceptor component from cal-ad ( $-42$  kcal mol<sup>-1</sup>) leads to an expected gas phase enthalpy value of  $-64$  kcal mol<sup>-1</sup> for pyridine reacting with the strong sites. The average enthalpy of  $-48$  kcal mol<sup>-1</sup> reported from the gas phase calorimetric study is lower than  $-64$  kcal mol<sup>-1</sup> consistent with the proposal that contributions from the second site are averaged in giving a low  $-\Delta H_{\text{AVE}}$ . It is interesting to note that the first few micromoles of pyridine corresponding to the first point in the gas–solid calorimetric titration of HZSM-5 give<sup>7c</sup> enthalpies of  $\sim -57$  kcal mol<sup>-1</sup>.

By using the procedures reported in our multiple equilibrium analysis of porous solids,<sup>19</sup> it may be possible to resolve sites 1 and 2, by carrying out gas phase calorimetric measurements over a series of temperatures. Each new temperature introduces new  $K$ 's, but the  $-\Delta H$  and  $n$ 's remain constant so the added enthalpy data will help define the system.

Consistent with the above discussion, the similarity in  $K$ 's for the different sites at high temperatures also prevent TPD, TGA, and DSC from resolving separate sites that differ substantially in strength, i.e., enthalpies. This adds to other reported complications involved in the use of these methods.<sup>6</sup>

An infrared study<sup>20</sup> of HZSM-5 (Si/Al ratio of 47) in the  $-\text{OH}$  stretching region with and without adsorbed aromatics showed a heterogeneity of the OH functionality. Variations in the Si–O and Al–O distances and the Si–O–Al bond angles as well as the immediate environment in the channel contribute to the differences in the acid strength of the sites. Spectral deconvolution gives five sites, compared to the three found by cal-ad titration with pyridine, lutidine, and 2,6-di-*tert*-butylpyridine. If there are five sites, calorimetry would group together sites whose enthalpies could differ by 1 or 2 kcal mol<sup>-1</sup>.

There is speculation in the literature,<sup>6c,8</sup> that elevated temperature are needed to access all of the Brønsted sites in HZSM-5. Binding base molecules to Brønsted sites is proposed to block access to other sites. The good agreement between the 0.6 mmol of sites found in our solution studies at room temperature and the 0.5 mmol of sites found in the gas phase studies of a similar HZSM-5 sample suggest the base migrates from site to site during the few second time scale of the room temperature, solution calorimetric measurement. After the instantaneous exotherm accompanying base addition, we do not observe the sloping base line that is expected for a reaction proceeding on the time scale of minutes. In NMR studies by these same authors<sup>8a</sup> who propose blocked access, it is claimed that site coverages less than one must be used to probe the Brønsted site with acetone to avoid complications<sup>11</sup> by exchange of chemisorbed or physisorbed species and bimolecular reactions.<sup>11</sup> At coverages less than 5 mmol g<sup>-1</sup> there is no proof that exchange is not occurring. Chemical shift anisotropies suggest that the exchange reaction could involve segmental motion or that some of the observed anisotropy is due the small contribution of sites 1 to 2. We conclude, in agreement with other literature reports,<sup>21</sup> that pyridine diffusion through all parts of the structure allows it to interact with all the acid sites relevant to catalysis.

The correlation of enthalpies of adduct formation to spectral changes in donor and acceptor molecules has been established for several solution systems.<sup>12</sup> Studies of spectral shifts in noncoordinating solvents has demonstrated a pronounced effect of the polarity of the medium in many instances.<sup>22</sup> The <sup>13</sup>C resonance of acetone, proposed to measure acid site concentration in zeolites, is consistent with 0.5 mmol g<sup>-1</sup> of the single acid sites found for HZSM-5 in gas phase calorimetry studies.<sup>8</sup> Consequently, the reported<sup>8</sup> <sup>13</sup>C shift of acetone does not discriminate among the differences in the donor–acceptor interaction involving sites 1 and 2. This could result from the sensitivity of the measurement or rapid exchange of acetone between the two sites or from dominant contributions to the shift by the polarity of the zeolite environment masking the differences in the specific interaction.

The difference in the <sup>13</sup>C shift of the  $\alpha$  and  $\beta$  carbons of mesityl oxide upon protonation has been used<sup>23</sup> to measure solution acidity. The  $\alpha$  proton is influenced slightly by protonation and is used to correct the  $\beta$ -shift for medium effects (i.e., nonspecific solvation in solution). In solution, rapid exchange and ion pairing gives rise to concentration dependent shifts which require extrapolation of the shift to infinite dilution. These shifts are expressed as  $H_0$  values using a calibration curve of  $\Delta\delta^\circ$  vs  $H_0$  values. In solids, the concentration of the strongest site must be large enough to detect. Furthermore, exchange with other strong sites and excess mesityl oxide must be slow

(20) Datka, J.; Boczar, M.; Gil, B. *Langmuir* **1993**, *9*, 2496.

(21) Redondo, A.; Hay, P. J. *J. Phys. Chem.* **1993**, *97*, 11754.

(22) Drago, R. S.; Hirsch, M. S.; Ferris, D. C.; Chronister, C. W. *J. Chem. Soc., Perkin Trans. 2* **1994**, 219.

(23) Farcasiu, D.; Ghenciu, A. *J. Am. Chem. Soc.* **1993**, *115*, 10901.

(19) McGilvray, J. M.; Drago, R. S. Submitted for publication.

on the NMR time scale, in order for the magnitude of this shift difference for site 1 to correlate to  $\Delta H$ .

Measurement of the temperature programmed desorption of isopropylamine from solid acids has been suggested as a means of measuring the quantity of Brønsted sites on a solid. Weakly bound amine is desorbed by heating at low temperatures. The amount of adsorbate undergoing acid catalyzed decomposition to give alkene and ammonia is reported to provide a measure of the number of strong acid sites. The values reported<sup>8</sup> for HZSM-5 correspond to the sum of  $n_1$  and  $n_2$ . If site 2 is a hydrogen bonding site, as cal-ad suggests, it is not expected to cause rearrangement. We propose that the porosity of the solid keeps the amine bound to site 2 as a reservoir for the acid catalyzed decomposition occurring at site 1. As alkene and ammonia form, they are desorbed and replaced on the Brønsted site by amine from site 2. In this manner the total amount of isopropylamine on site 1 and 2 reacts. Any loosely held excess amine is volatilized before degradation temperatures are attained. Providing a reservoir of substrate would be an important advantage of using zeolites in catalysis.

**Relationship of Cal-Ad and NMR Results.** Solid-state NMR has been used extensively to probe the reactivity of zeolites and is very important for the characterization of different preparations. <sup>1</sup>H, <sup>29</sup>Si, and <sup>27</sup>Al MAS-NMR spectra of our sample of HZSM-5 are given in Figure 2. The proton spectrum shown in Figure 2a is resolved into three peaks (see Experimental Section) that are assigned to bridging (AlOH) hydroxyl groups (at 4.0 ppm), hydroxyl groups attached to extraframework aluminum (at 2.5 ppm), and silanol groups (at 1.7 ppm). These assignments are made on the basis of literature reports.<sup>13</sup> The resolved <sup>1</sup>H signal for the bridging (AlOH) at 4 ppm accounts for 27.6% of the total proton spectral area. The resolved silanol peak accounts for 27.3% of the proton spectra giving a bridging framework AlOH to silanol ratio of one. The peak assigned to extraframework aluminum has a peak area of 37.5% of the signal. A very broad peak results at 6.2 ppm corresponding to 7.6% of the spectral intensity.

The <sup>27</sup>Al MAS-NMR spectrum of the HZSM-5 (Figure 2b) provides information about framework and nonframework aluminum in the zeolitic structure. Curve resolution shows two lines at 54 and 0 ppm due to four-coordinated framework and six-coordinated extraframework aluminum, respectively. An additional broad line appears at about 32 ppm which is related to tetrahedral extraframework Al-OH.<sup>13a,b</sup> The peak areas indicate 29.1% extraframework aluminum (lines at 0 and 32 ppm) and 70.9% of framework aluminum (line at 54 ppm). With a bulk Si/Al atomic ratio of 36, the ratio of silicon to framework aluminum atoms is 50.8. An HZSM-5 sample studied by gas solid calorimetry<sup>8d</sup> has 79% framework aluminum in a sample with a bulk Si/Al ratio of 54 and a silicon to framework aluminum ratio of 68.

The number of framework aluminums per unit cell and per gram of solid can be calculated using the unit cell formula for HZSM-5 (H<sub>7</sub>Al<sub>7</sub>Si<sub>96-n</sub>O<sub>192</sub>) and the framework Si/Al ratio. For every 50.8 silicons there is one aluminum giving an empirical formula of H<sub>1.9</sub>Al<sub>1.9</sub>Si<sub>94.1</sub>O<sub>192</sub> for our sample. In order to compare NMR results with cal-ad results, it would be useful to know the acid site density in mol per gram of HZSM-5 zeolite. Assuming all the framework aluminums lead to acid sites, the site density is obtained by dividing moles of aluminum per unit cell by the MW of the unit cell. This leads to  $0.32 \pm 0.05$  mmol of acid sites per gram. Since the intensity of the resonance assigned to the AlOH sites in the <sup>1</sup>H MAS-NMR spectrum is similar to that assigned to the silanol groups, there also are 0.32 mmol of silanols per gram.

None of the strongest sites arise from extra lattice material.  $\gamma$ -alumina is the most acidic form of alumina, and its strongest sites are  $\sim -18$  kcal mol<sup>-1</sup>. Thus, nonframework alumina will have little impact on the cal-ad or catalysis results and at most will block some sites and influence the  $n$ -value.

The <sup>29</sup>Si MAS-NMR spectrum (Figure 2c) shows silicon environments<sup>13</sup> assigned to structurally nonequivalent silicon atoms bonded to other silicons Si(OAl) (i.e., no aluminum attached) at -117.0 and -113.2 ppm. These resonances constitute 14.1% and 71.4%, respectively, of the total silicon resonance. The Si(1Al) and Si(OAl, 1OH) defect sites have almost identical chemical shifts leading to one resonance whose resolved contribution is 14.1% of the silicon resonance. The Si(1Al) sites are bound to the acidic hydroxyl aluminum centers and are present in a 1:1 ratio to the silanol Si(OAl, 1OH) sites. With four silicons bound to each of the 1.9 aluminums in the unit cell, there are 7.6 Si(1Al) and 7.6 Si(OAl, 1OH) per unit cell.

With half the area of the -107.3 ppm resonance or 7.0% of the total silicon resonance due to Si(1Al), the Si/Al framework ratio is given by  $100 / (0.25 * 7.03)$  or 56.9 (see Experimental Section). This result agrees, within experimental error of the resolution, to that obtained from <sup>27</sup>Al MAS-NMR. The silanol groups correspond to isolated Si-OH functionality with cal-ad enthalpies of binding expected<sup>10b</sup> to be  $<5$  kcal mol<sup>-1</sup>.

The significant aspect of this analysis is that only 19% of the framework AlOH sites lead to the 0.05 mmol of strong acid sites. The total of the acid sites from cal-ad ( $n_1 + n_2$ ) equals  $0.6 \pm 0.2$  mmol per gram which is in reasonable agreement with the  $0.3 (\pm 0.2)$  mmol of framework aluminum from NMR. Thus, both sites 1 and 2 for the pyridine reaction arise from bridging Al(OH)Si functionality. Our Si and Al NMR spectra do not distinguish the two types of acid centers arising from framework AlOH groups, and unless the very broad proton resonance at 6.2 ppm is due to site 1, proton NMR does not distinguish them. It is significant, that <sup>1</sup>H NMR over a range of temperatures probing dipolar coupling to <sup>27</sup>Al show two potential Brønsted environment.<sup>24</sup>

## Conclusions

The application of the cal-ad method to HZSM-5 extends the enthalpy criterion used to measure solution acidity to zeolites. As in solution, the donor-acceptor component, which is related to bond strength, is best reflected by the enthalpy.<sup>12</sup> The donor-acceptor component is determined, and the enthalpy scale from cal-ad provides a temperature independent scale of acidity that establishes HZSM-5 as a strong acid but not a superacid.

Study of the reaction of pyridine with HZSM-5 by cal-ad shows that the 0.6 mmol of Brønsted sites found with other methods are really 0.0415 mmol of a strong Brønsted site,  $-\Delta H = 42.1 \pm 0.8$  kcal mol<sup>-1</sup> and 0.53 mmol of a weaker hydrogen bonding site,  $-\Delta H = 8.6 \pm 3.8$  kcal mol<sup>-1</sup>. For the first time a solid acidity is characterized by  $K$ ,  $n$ , and  $\Delta H$ . This characterization proves that both sites react simultaneously even at lower base concentration. The similarity expected for the  $K$ 's at high temperatures accounts for the sites not being distinguished by gas phase calorimetry or temperature programmed desorption measurements.

Cal-ad studies of the reactions with pyridine, 2,6-lutidine, and 2,6-di-*tert*-butylpyridine show all of the strong acid sites, and most of the weaker sites ( $-9$  kcal mol<sup>-1</sup>) are located in

(24) (a) Haw, J. F.; Nicholas, J. B.; Xu, T.; Beck, L. W.; Ferguson, D. B. *Acc. Chem. Res.* **1996**, *29*, 259. (b) Beck, L. W.; White, J. L.; Haw, J. F. *J. Am. Chem. Soc.* **1994**, *116*, 9657.



pockets or corners that exist in the zig-zag, 5.5 Å channel of the zeolite. In addition to surface sites, hydrogen bond sites exist in the straight channels that can be accessed by 2,6-lutidine. Neither the surface sites nor straight channels contain measurable quantities of Brønsted sites.

The cal-ad results reported in this article are shown to be consistent with reported experimental observations of zeolite reactivity. Reasons are offered that explain why most of the indirect methods for estimating acidity do not discriminate sites  $n_1$  from  $n_2$  even though enthalpies of binding differ by  $\sim 30$  kcal mol<sup>-1</sup>. As a result, an overestimate of the number of strong Brønsted sites in the solid exists in literature reports. The

hydrogen bonding sites are suggested to play a role in reactivity by providing a reservoir for reaction at the Brønsted sites.

**Acknowledgment.** Sílvia C. Dias is grateful to CNPq (Conselho Nacional de Desenvolvimento Científico e Tecnológico) for the grant (proc. 200870/93-9) of a scholarship for pursuing Ph.D. at the University of Florida and the Universidade de Brasília for the leave of absence during this period. PQ Corporation is acknowledged for providing HZSM-5. Discussion of the NMR results with Dr. Mickel Anderson is also appreciated.

JA9633530